Impact of exhaust gas fuel reforming and exhaust gas recirculation on particulate matter morphology in Gasoline Direct Injection Engine

Bogarra Macias, Maria; Herreros, Jose; Tsolakis, Athanasios; York, Andrew; Millington, Paul; Francisco, Martos

DOI:
10.1016/j.jaerosci.2016.10.001

Document Version
Peer reviewed version

Citation for published version (Harvard):
Bogarra Macias, M, Herreros, J, Tsolakis, A, York, A, Millington, P & Francisco, M 2017, 'Impact of exhaust gas fuel reforming and exhaust gas recirculation on particulate matter morphology in Gasoline Direct Injection Engine', *Journal of Aerosol Science*, vol. 103, pp. 1-14. https://doi.org/10.1016/j.jaerosci.2016.10.001

www.elsevier.com/locate/jaerosci

Impact of Exhaust Gas Fuel Reforming and Exhaust Gas Recirculation on Particulate Matter Morphology in Gasoline Direct Injection Engine

M. Bogarra, J.M. Herreros, A. Tsolakis, A.P.E. York, P.J. Millington, F.J. Martos

PII: S0021-8502(16)30065-9
DOI: http://dx.doi.org/10.1016/j.jaerosci.2016.10.001
Reference: AS5052

To appear in: *Journal of Aerosol Science*

Received date: 1 March 2016
Revised date: 29 July 2016
Accepted date: 4 October 2016

Cite this article as: M. Bogarra, J.M. Herreros, A. Tsolakis, A.P.E. York, P.J. Millington and F.J. Martos, Impact of Exhaust Gas Fuel Reforming and Exhaus Gas Recirculation on Particulate Matter Morphology in Gasoline Direct Injectio E n g i n e , *Journal of Aerosol Science* http://dx.doi.org/10.1016/j.jaerosci.2016.10.001

Impact of Exhaust Gas Fuel Reforming and Exhaust Gas Recirculation on Particulate Matter Morphology in Gasoline Direct Injection Engine

M. Bogarra[a], J.M. Herreros[a], A. Tsolakis[a*], A.P.E. York[b], P.J. Millington[b], F.J. Martos[c]

[a]*School of Mechanical Engineering, University of Birmingham, Edgbaston, B15 2TT, UK*

[b]*Johnson Matthey Technology Centre, Blount's Court, Sonning Common, Reading, RG4 9NH, UK*

[c]*Department of Mechanical, Thermal and Fluids Engineering, University of Málaga, 29071, Málaga, Spain*

Abstract

Modern Gasoline Direct Injection (GDI) engines offer increased power output, improved fuel economy and reduced CO_2 emissions. However, the increased particulate matter (PM) emission level still remains a challenging task. Understanding PM features such as morphological and microstructural parameters through transmission electron microscopy can provide information about their formation, filtration and soot oxidation processes in the gasoline particulate filters and their impact on human health. This research article characterises PM emitted from a 2L 4-cylinder GDI engine at two injection timings: i) ECU settings which produces PM with high volatile content and ii) advanced injection timing to increase soot formation rate. Primary particle size distributions formed by volatile nature PM, present a higher standard deviation than for the sooty PM, while the former ones presented higher fractal dimension. In addition, five different methods of est*i*mating PM fractal dimension reported in the GDI literature have also been compared and it was concluded that the arising trends were in agreement. The effect of high percentages of exhaust gas recirculation (EGR) and reformate gas combustion on PM characteristics have been analysed. EGR does not have a significant effect in PM morphology. On the other hand, reformate combustion reduces the size of the primary particle and the agglomerates as well as increasing the fractal dimension.

Keywords: Particulate matter, fuel reforming, soot morphology, Gasoline Direct Injection, Transmission Electron Microscope

DEFINITIONS, ACRONYMS, ABBREVIATIONS

A	Projected area.
A_p	Primary particle area
α	Exponential Factor
bTDC	Before Top Dead Centre

CAD	Crank Angle Degree
CBM	Counting Box Method
D_f	Fractal Dimension
DPF	Diesel Particulate Filter
d_{p0}	Primary particle diameter
ECU	Electronic Computer Unit
EGR	Exhaust Gas Recirculation
GDI	Gasoline Direct Injection Engine
GPF	Gasoline Particulate Filter
HCs	Hydrocarbons
TEM	Transmission Electron Microscope
k_f	Pre-factor or structural coefficient
L	Length of the rectangle containing the minimum area of particle
m	number of pixels per aggregate
NEDC	New European Driving Cycle
n	Number of primary particles
PM	Particulate Matter
PSD	Particle Size Distribution
R_g	Radius of gyration
r_i	distance between each pixel and the centroid of soot aggregate
REGR	Reformated Exhaust Gas Recirculation
RFF	Root Form Factor
SPSS	Statistical Package for Social Sciences
W	Width of the rectangle containing the minimum area of particle

1. Introduction

The introduction and development of the modern Gasoline Direct Injection (GDI) engines in recent years offer several advantages, such as improved efficiency, reduced fuel consumption and CO_2 emissions, compared with previous gasoline technologies. On the other hand, injecting the fuel directly into the combustion chamber leads to high probability of creating fuel-rich regions due to wall/piston wetting that are known to be the origin of particulate matter (PM) formation. GDI engines are reported to increase significantly PM emissions

compared to their Port Fuel Injection counterparts (Zhang et al., 2012) and to diesel equipped with Diesel Particulate Filters (DPFs) (Badshah et al., 2015). Transmission electron microscope (TEM) has been largely used for PM characterisation, including size, shape and microstructure will provide an understanding of their potential impact to human health and environment (Barone et al., 2012; Broday et al., 2011; Farron et al., 2011; Gaddam et al., 2013; Karjalainen et al., 2014; La Rocca et al., 2015; Uy et al., 2014).

For diesel engines, the importance of PM morphological parameters as well as the link of PM with human health has been broadly investigated. For instance, the porosity and permeability are related to the diameter and the number of primary particles. The fractal dimension is directly linked with the volume arrangement of the agglomerates and it has been reported that the higher fractal dimension increases the effective density of PM (Broday et al., 2011). In order to accomplish the Euro6c, Gasoline Particulate Filter (GPF) systems might be required and similarly to Diesel Particulate Filters for the optimisation of filter regeneration events, soot morphology must be accurately characterised (Lapuerta et al., 2010; Vander Wal et al., 2007). Also, the residence time of PM in the atmosphere and the rate of deposition on human body depends on soot morphology, in particular size and specific surface area (Giechaskiel et al., 2009; Löndahl et al., 2009), which are related with the dose and the inflammatory response of PM exposition, as it has already been seen in diesel engines (Giechaskiel et al., 2009). Fiorito et al. observed higher cytotoxicity and oxidative potential in particles emitted under low emission conditions (i.e. Euro IV) compared to older diesel vehicles (pre-Euro standard). Special attention must be paid then for the upcoming legislations. (Fiorito et al., 2011). This new knowledge will allow targeting engine conditions with lower PM emissions or with PM characteristics more favourable for filter regeneration and therefore, the design of more efficient aftertreatment systems.

There are limited studies reporting a complete PM morphological analysis (i.e. primary particle diameter, fractal dimension) for GDI engines. So far in the literature, the studies available are limited to the influence of engine speed, load, air-fuel ratio and ethanol combustion on particle morphological characteristics. However, the effect of exhaust gas recirculation (EGR) or hydrogen combustion has not been reported conversely to diesel engines (Al-Qurashi et al., 2008; Lapuerta et al., 2007). The following paragraphs review the morphology studies in GDI engines.

PM nature

Barone et al. (Barone et al., 2012) studied PM characteristics for a fuel blend composed of 20% ethanol and 80% commercial gasoline in a 4-cylinder 2L direct injection spark ignition. Particles were directly collected from the engine exhaust and the agglomerates were analysed using TEM. They reported the presence of the different types of PM agglomerates (i) fractal-like particles (similar to diesel agglomerates), (ii) hydrocarbon (HC) droplets and (iii) small agglomerates composed of very small primary particles (d_{p0}=6 nm). Particles of different nature were also reported by Karjalainen et al. (Karjalainen et al., 2014). The study was carried out using a 2011 GDI engines powered with commercial gasoline (ethanol quantity below 10%) during the New European Driving Cycle (NEDC). Nearly spherical particles with diameters spanning from 10nm to 200nm as well as diesel-like agglomerates were reported. The analysis of composition of fractal-like particles showed the presence of metals, which originated in the engine oil. The HC droplets were mainly composed of elemental carbon, although some traces of the oil metals were also present. Small spherical soot particles were also found similarly to Barone et al. (Barone et al., 2012).

Diameter of primary particles

conversely to diesel engines, researchers have reported different ranges for primary particle diameter (d_{p0}). For instance, Uy et al. (Uy et al., 2014) stated an average primary particle diameter of 23nm, while La Rocca et al. (La Rocca et al., 2015) reported an average value of 36 nm. In addition La Rocca et al. observed more spherical shape primary particles from the GDI combustion compared to diesel. Both Barone et al. (Barone et al., 2012) and Gaddam et al. (Gaddam et al., 2013) reported a wide range of primary particle diameters spanning from 7 to 65 nm. A similar range (from 5 – 60 nm) is reported in (Miyashita et al., 2015) under advanced and retarded injection timings. In Lee et al. (Lee et al., 2013), the same range and the presence of small spherules with an ethanol-gasoline blend (E20) were noted at different equivalence ratios and fuel injection timings. It was concluded that PM emitted from GDI engines has a higher number of small primary particles compared to the ones emitted from diesel combustion. Those small particles have an amorphous nanostructure, suggesting that they are nascent particles which have not gone under a further graphitization process (Lee et al., 2013). On the other hand, Uy et al. (Uy et al., 2014) reports the existence of an even narrower range of primary particles with a minimum size of 8.3 nm, maximum size of 43.3 and 7.5 nm standard deviation. As the range of primary particles sizes in GDI engines is wider than in diesel, an analysis of primary particle distribution instead of just the mean diameter is needed.

Fractal dimension

most of the studies to date confirm that PM chain-like agglomerates are present under GDI combustion, similarly to diesel agglomerates. Wang-Hansen (Wang-Hansen et al., 2013) found aciniform-shape particles in scanning electron microscope micrographs. The particles fractal dimension can be used as a tool to predict the impact of inhaled particles on human health (Broday et al., 2011) and to guide the design of novel efficient aftertreatment systems for PM control. It quantifies the shape of fractal geometries (self-similarity) which means that the objects will be the same after scale transformation (Schaefer, 1988). PM aggregates are considered as fractal-like structures (Maricq, 2007) , thus fractal dimension (D_f) is commonly used to describe the shape of the particles and their reactivity and aero-dynamical behaviour (Wentzel et al., 2003). Ranges of parameters and methods have been used to quantify the shape of chain-like PM agglomerates. Similarly to diesel PM agglomerates, D_f has mostly been used to quantify the PM shape from GDI engines. Seong et al. (Seong et al., 2013) used a logarithmic method to calculate the PM fractal dimension and they obtained values between 1.74 (190 CAD bTDC injection timing) and 1.8 (330 CAD bTDC injection timing) which lies between the D_f from light- and heavy-duty diesel engines (Seong et al., 2013). La Rocca et al. (La Rocca et al., 2015) obtained an average value of 1.44 which is below the reported average D_f. Gaddam et al. (Gaddam et al., 2013) used the iterative method described in Lapuerta et al. (Lapuerta et al., 2006) and they reported that the fractal dimension was in the range of 1.69 and 2.39 depending on the engine operating condition. The root form factor (RFF) has been used in (Gaddam et al., 2013) to quantify the shape of the agglomerates. This parameter is calculated as the ratio between area and perimeter, thus, it can be comparable to the fractal dimension meaning. RFF values between 0.29 and 0.33 were obtained.

Engine operating condition effect in morphological parameters

The influence of the engine operating conditions on PM primary particle size has also been discussed in the literature. Lee et al. (Lee et al., 2013) studied the effects of fuel injection timing and equivalence ratio on average primary particle diameter, but they found no significant differences and confirmed the existence of primary particles with a broad range of diameters. In a different study by the same authors (Seong et al., 2013), the effect of injection timing and engine load on PM morphology was investigated. As the fuel injection timing was advanced, d_{p0} and the radius of gyration (R_g) increased gradually from 20 to 29 nm and 66 to 90 nm respectively. d_{p0} changed linearly with the engine load, but this trend was also

dependant on the engine speed. The most influential parameter that affects the fractal dimension was found to be the local fuel/air ratio and was ranging from D_f of 2.38 for rich condition, 2.20 for the late end of injection and 2.06 for high load condition (Gaddam et al., 2013). This trend is in agreement with the larger amount of nuclei produced due to these rich-fuel regions and therefore, more agglomeration chances. On the other hand, for lean combustion D_f was 1.86 and for stoichiometric combustion the lowest value of 1.69 was obtained.

Hydrogen combustion in gasoline can be a possible way to reduce PM (Bogarra et al., 2016; Fennell et al., 2014) by slowing down the rate of soot production and enhance soot oxidation due to the formation of OH radicals as previously reported (Fennell et al., 2013; Stone et al., 2010). Moreover, its physicochemical properties, such as higher flame velocity and less quenching gap can improve engine thermal efficiency (Akif Ceviz et al., 2012; Verhelst et al., 2009). A feasible method is the catalytic production of hydrogen via on-board exhaust gas reforming. This technique, known as reformed exhaust gas recirculation (REGR), recovers waste heat from the exhaust to heat up a catalyst that utilizing water and CO_2 from the exhaust promote chemical reactions whose products are mainly hydrogen and CO. For this investigation, an on-board prototype fuel reformer provided by Johnson Matthey and consisting of five metallic plates coated with Pt – Rh was used. The benefits of REGR in GDI engines in terms of fuel economy, engine stability, higher dilution rates achieved and PM have been previously analysed in (Bogarra et al., 2016; Fennell et al., 2014; Fennell et al., 2015; Fennell et al., 2013) A different approach to produce on-board reformate is dedicated EGR, developed by the Southwest Research Institute (Alger et al., 2009). The exhaust of a dedicated cylinder is operated rich to reform fuel into CO and H_2. This cylinder provides all the reformulated exhaust gas back to the intake manifold. Introducing the EGR directly to the intake manifold faces the control and tolerance challenges associated to EGR. In order to promote H_2 and CO production, a partial oxidation catalyst is included in the loop (Alger et al., 2009). Use of the dedicated EGR has been reported to increase the engine efficiency by at least 10% (Chadwell et al., 2014) and to simultaneously reduce engine out NOx emissions in the range of 40%-80% (Henry et al., 2016). However, the effect of dedicated EGR on PM is dependent on the engine operating condition and no clear trends have been found (Henry et al., 2016).

Despite EGR, hydrogen combustion and REGR have been found to be beneficial for fuel economy and to reduce NOx in GDI engines, no studies of PM morphology have been

performed. In this investigation a comprehensive morphological analysis of PM emissions emitted by a Euro 5 4-cylinder GDI engine was carried out. The influence of EGR and REGR on the primary particle diameter, number of particles per agglomerate and radius of gyration were studied at two different fuel injection timings, one that produced PM with high volatile organic content and one that promoted soot formation. Furthermore, the fractal dimension is assessed with different methods typically used in the literature.

2. Experimental setup and methodology

2.1.Experimental setup

The engine used for this study is a 2 L, 4-cylinder, side-mounted injector, air-guided GDI. A steady-state condition corresponding to a medium-load point of the NEDC was selected: 2100±2 rpm and 4.7±0.3 bar indicated mean effective pressure. The details of the engine specification can be found in Table 1. Standard EN228 gasoline with 5% (v/v) ethanol content provided by Shell has been used for this research. Fuel properties are presented in Table 2.

Table 1. Engine specifications.

Compression Ratio	10:1
Bore x Stroke	87.5 x 83.1 mm
Turbocharger	Borg Warner K03
Rated Power	149 kW At 6000 rpm
Rated Torque	300 Nm At 1750-4500 rpm
Engine Management	Bosch Me17

Table 2. Gasoline properties.

Analysis (Test method)		Unit	Result
Density at 15ºC (DIN EN ISO 12185)		kg/m^3	743.9
Distillation (DIN EN ISO 3405)	IBP	ºC	34.6
	20% v/v	ºC	55.8
	50% v/v	ºC	94.0
	FBP	ºC	186.3
C		m/m %	84.16
H		m/m %	13.48
O		m/m %	2.36
Paraffins		% vol	43.9
Olefins		% vol	11.7
Naphthenes		% vol	7.8
Aromatics		% vol	26.9
Oxygenates		% vol	7.7
Sulfur		ppm	6
Lower Heating Value (DIN 51603-1)		MJ/kg	42.22
MON (DIN EN ISO 5163)		85.3	85.3
RON (DIN EN ISO 5164)		96.5	96.5

For the PM morphology analysis 3.05 mm TAAB Formvar coated copper grids were loaded directly in the engine exhaust pipe before the three way catalytic converter. A JEOL 1200EX TEM LaB6 80 keV operating voltage and capable of loading two grids was selected for this purpose. It has been stated in (Lee et al., 2013; Uy et al., 2014) that the energy of the electron beam could alter the morphology and evaporate part of the HCs adsorbed on the particles. To avoid these effects, especially at 303 CAD bTDC where the HC concentration is high, a microscope with lower operating voltage was employed.

2.2.Test procedure and methodology

2.2.1. Engine conditions

Morphological analysis of GDI particles emitted at high rates of EGR and REGR compared to noEGR condition has been carried out. In order to study the change in morphology for different types of PM two injection timings producing i) small soot nuclei and volatile organic compounds (303 CAD bTDC, ECU settings) and ii) highly sooty particles (335 CAD bTDC, advanced injection setting) have been analysed. In a previous work (Bogarra et al., 2016), it was reported that advanced injection settings produced ten times higher PM concentration. Further analysis of PM nature at both injection timings was performed. Thermogravimetric analysis showed that 98% of PM emitted is soot under early injection timing.

The maximum percentage of EGR tolerated by the engine, which maintained the coefficient of variation (COV) below 5%, was used for the analysis: 19% and 24% for 303 CAD bTDC and 335 CAD bTDC, respectively. In order to compare the REGR with EGR, the same dilution rates were utilised. The maximum position of the in-cylinder pressure was maintained in a ±3 CAD narrow window for EGR and REGR according to the baseline maximum peak position. These combustion settings are summarized in Table 3 where the percentage of EGR/REGR, spark timing per condition and the maximum peak pressure position compared to the baseline are reported. 200 cycles were considered for obtaining these values.

Table 3. Engine settings for noEGR, EGR and REGR at both injection timings: 303 and 335 CAD bTDC.

Injection timing	Dilution	Spark timing (CAD bTDC)	COV of IMEP (%)	IMEP	Position Pmax (CAD)
303 CAD bTDC	noEGR	+ 24 (ECU)	2.03	4.7	16
	EGR (19%)	+ 32.25 (+ 8.25*)	4.35	4.71	16

335 CAD bTDC	REGR (19%)	+ 27.75 (+ 3.75*)	3.33	4.62	16
	noEGR	+ 24 (ECU)	1.2	4.71	12
	EGR (24%)	+ 41.25 (+ 17.25*)	5.22	4.69	12
	REGR (24%)	+ 23.25 (- 0.75*)	2.97	4.63	12

(*) + advance, - retard, spark timing with respect to ECU settings.

Prior to the test, the engine was warmed up, and the measurements started when 95±0.5 °C coolant and 101±2 °C oil temperatures were achieved. The charge air temperature was maintained at 40±2 °C during the whole experiment. Fuel injection pressure and fuel injection rail temperature were maintained constant at 60±2 bar and 75.5±0.5 °C, respectively for both injection timings.

2.2.2. PM morphological analysis

The accurate estimation of the diameter of the primary particle is crucial as the rest of the morphological parameters are derived from it. The common method to obtain d_{p0} is by manual measurements on account of the difficulties in identifying the primary particles boundaries in the agglomerates. In (Kondo et al., 2013), it is claimed that both the operator and the position of the agglomerate in the TEM grid are influential in the precision of the diameter dimension. Therefore, the size of the sample must be large enough to assure its normality. With this aim, at least 180 primary particles per condition were considered, distributed in 15 different agglomerates randomly located in the TEM grid. (Gaddam et al., 2013) discusses whether d_{p0} can be fitted to a log-normal distribution. One-sample non-parametric Kolmogorov Smirnov test in IBM statistical package for social sciences (SPSS) software was performed to check the log-normality. Furthermore, to numerically evaluate the statistical differences between the conditions (i.e. noEGR vs. EGR, noEGR vs. REGR and EGR vs REGR), a T-test has been executed.

The number of primary particles refers to the number of single spherules-like that can be found in a selected aggregate. It can be calculated as in Equation [1].

$$n = \left(\frac{A}{A_p}\right)^{\alpha} \quad [1]$$

Where:

n is the number of primary particles.

A is the projected area from the micrograph.

A_p is the area of the primary particle considered as a circle $A_p = \frac{\pi}{4} d_{p_0}^2$

α is the exponential factor for particle overlap. Its value has been assumed to be 1.09 (Lee et al., 2013; Zhu et al., 2005).

The Radius of gyration can be estimated as (Filippov et al., 2000; Kondo et al., 2013; Lapuerta et al., 2006).

$$R_g = \sqrt{\frac{1}{m}\sum r_i^2} \quad [2]$$

Where:

m is the number of pixels per aggregate.

r_i is the distance between each pixel and the centroid of soot aggregate (nm).

D_f has been widely estimated from TEM micrographs however, particle overlapping and the cluster anisotropy (Van Gulijk et al., 2004; Wentzel et al., 2003) can result in misleading values. In order to obtain the D_f, several methods and equations have been proposed in the literature. The most widely method is calculating the gradient of Equation 3, known as fractal-equation (Wozniak et al., 2012) or power law relationship (Lapuerta et al., 2006; Lottin et al., 2013). However, it has to be considered that this equation is only valid for agglomerates with self-similarities and therefore, the properties of the agglomerate are not scale variant, (Theiler, 1990; Wozniak et al., 2012).

$$\mathrm{In}(n) = \mathrm{In}(k_f) + D_f \mathrm{In}\left(\frac{R_g}{d_{p_0}}\right) \quad [3]$$

Where k_f is the pre-factor or structural coefficient (Wozniak et al., 2012).

In this work, five different methods to quantify the shape of the agglomerates have been compared: i) a widely used logarithm method from (Zhu et al., 2005), ii) logarithm method using the square root of the product LW (length and width of the rectangle containing the minimum area) defined in (Wozniak et al., 2012), iii) counting box method (CBM) described in (Lottin et al., 2013; Wozniak et al., 2012), iv) iterative method described in Lapuerta et al. (Lapuerta et al., 2006), and v) root form factor (Gaddam et al., 2013). The first four methods calculate the fractal dimension, while the last method is a non-dimensional parameter based on the ratio area-perimeter, being comparable to fractal dimension, Equation 4.

$$RFF = \sqrt{\frac{4\Pi A_p}{Perimeter^2}} \quad [4]$$

Prior to the morphological analysis, the TEM images were pre-treated using commercial software. This pre-treatment consists of background removal and contrast increase to facilitate the primary particle recognition. Furthermore, an in-house MATLAB code has been developed for calculating morphological parameters including diameter of primary particle , number of primary particles per agglomerate, radius of gyration as well as fractal dimension and RFF. Similar codes have been generated extensively in the soot characterization literature (Kondo et al., 2013; Ruiz et al., 2015; Zhu et al., 2005).

3. RESULTS AND DISCUSSION

3.1. Particulate matter patterns

A sample of the TEM micrographs of the particles collected from the GDI engine exhaust at the manufacturer ECU fuel injection timing settings (303 CAD bTDC) are shown in Figure 1. Four different kinds of particles were identified: a) a nearly-spherical HCs droplets, b) large agglomerates composed of small primary particles c) diesel-like particles with the presence of HCs on them and d) 'dry' diesel-like particles. The presence of the different types of particles is in agreement with the work presented in (Barone et al., 2012; Karjalainen et al., 2014) during steady-state engine operation and vehicle under NEDC, respectively. Also, the presence of small spherical particles of around 6 nm is found according to the work described in (Barone et al., 2012; Gaddam et al., 2013; Seong et al., 2013).

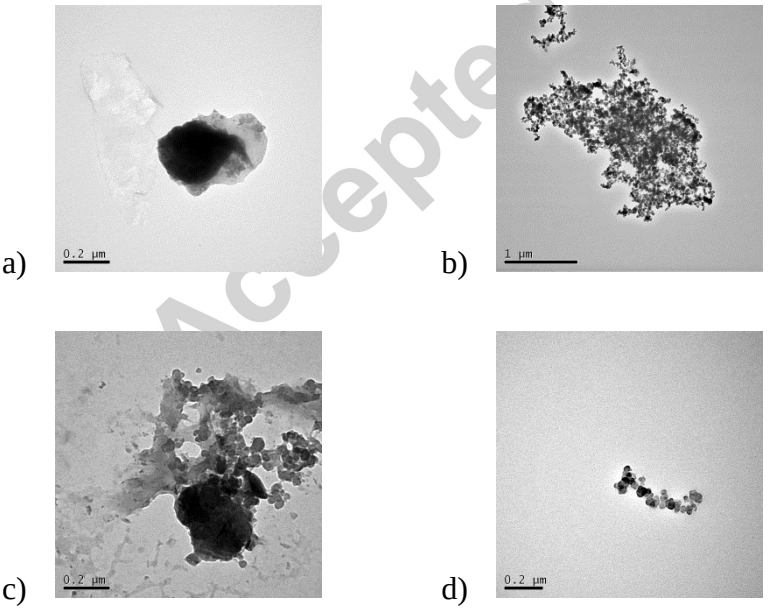

Figure 1. TEM micrographs of PM for 303 CAD bTDC: a) Near-spherical droplets b) Large agglomerates c) wet diesel like-particle and d) diesel-like particles

In the engine condition with advanced injection timing (335 CAD bTDC), the collected particles were classified as 'dry' diesel-like particles (Figure 2). This is due to increased likelihood of wall and piston wetting creating a high amount of locally fuel rich regions.

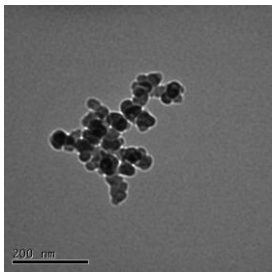

Figure 2. TEM micrographs for advanced injection timing settings.

3.2. Morphology parameter analysis of agglomerates

3.2.1. Primary particle diameter analysis

The log-normality of the measured d_{p0} was statistically analysed using IBM SPSS statistics (Table 4). The majority of the studied conditions presented a log normal distribution with significance higher than 0.05. However, the primary particles measured for EGR and REGR at 303 CAD bTDC were not normally distributed (i.e. significance level <0.05) and cannot be considered for analysis. It is thought that this is a result of the 'multi-modal' nature primary particle size distribution rather than a typical 'uni-modal' distribution from diesel (Wentzel et al., 2003) and some GDI combustion regimes (Gaddam et al., 2013; La Rocca et al., 2015). Therefore, the primary particle size distributions and morphological parameter results for EGR and REGR for 303 CAD bTDC are not shown as they cannot be fitted to a log-normal distribution. In Figure 3, a micrograph per condition has been given as an example. It can be observed how the nature of the particles changes from soot to HCs when the injection is retarded and EGR or REGR were used.

Table 4. Statistical normality tests.

	Null Hypothesis	Test	Significance	Decision
1	The distribution of log(335baseline) is normal with mean 3.289 and standard deviation 0.23	One-sample kolmogorov-smirnov test	.131[1]	Retain the null hypothesis
2	The distribution of log(303baseline) is normal with mean 3.386 and standard deviation 0.23	One-sample kolmogorov-smirnov test	0.200[1]	Retain the null hypothesis
3	The distribution of log(335EGR) is normal with mean 3.147 and standard deviation 0.26	One-sample kolmogorov-smirnov test	0.200[1]	Retain the null hypothesis

4	The distribution of log(335REGR) is normal with mean 3.24 and standard deviation 0.31	One-sample kolmogorov-smirnov test	0.097[1]	Retain the null hypothesis

Asymptotic significance are displayed. The significance level is 0.05.

[1] Lilliefors Corrected

a)

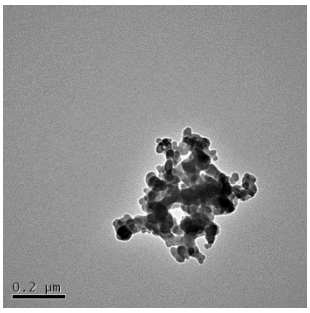

b)

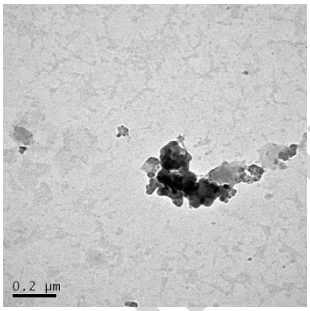

c)

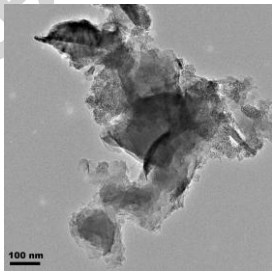

d)

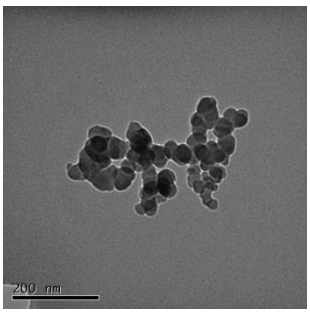

e)

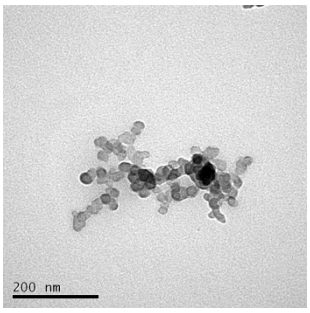

f)

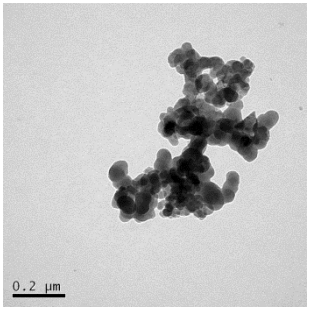

Figure 3. Example of micrographs for the different condition studied: 303 CAD bTDC a) noEGR b) EGR c) REGR, 335 CAD bTDC d) noEGR e) EGR and f) REGR.

Figure 4 shows the primary PSD for noEGR at the two injection timings. The engine operation with 303 CAD bTDC injection timing presented a wider size distribution of PM emissions (i.e. higher variability in the primary particle size). The different types (Figure 1) seen from this injection timing can be the reason for this wider distribution. The lower time available for air-fuel mixing can lead to the presence of these unburnt small particles and reduce the time for PM graphitization and structure reorganization, as suggested in (Lee et al., 2013), resulting in the formation of less compact primary particle and therefore presenting larger diameters. On the other hand, the 335 CAD bTDC fuel injection timing decreased the primary particle diameter and led to narrower distribution.

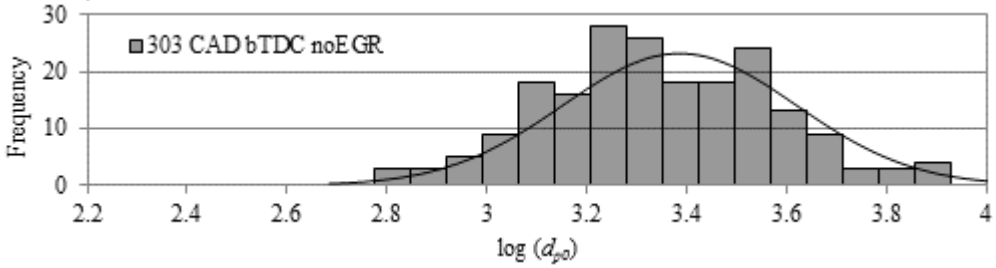

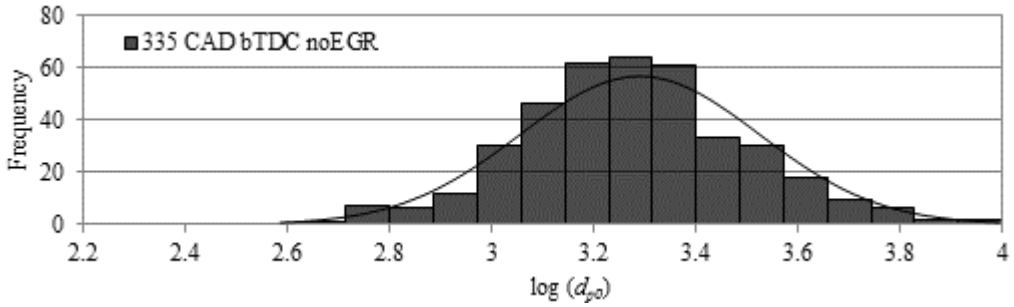

Figure 4. Primary particle size distributions for the baseline at both fuel injection timings: 303 and 335 CAD bTDC.

In Figure 5, the influence of EGR and REGR at 335 CAD bTDC is analysed. It can be observed, that EGR tends to shift the particle distribution to smaller sizes. The reduction in diameter observed under EGR conditions is also in agreements with the results reported in (Hedge et al., 2011). The authors attributed this behaviour to the EGR capability of inhibiting PM nucleation. Although post-flame temperature is decreased with EGR operation and therefore, agglomeration could be increased, it seems that nucleation inhibition overcomes reduced post-flame temperature effects (Hedge et al., 2011).

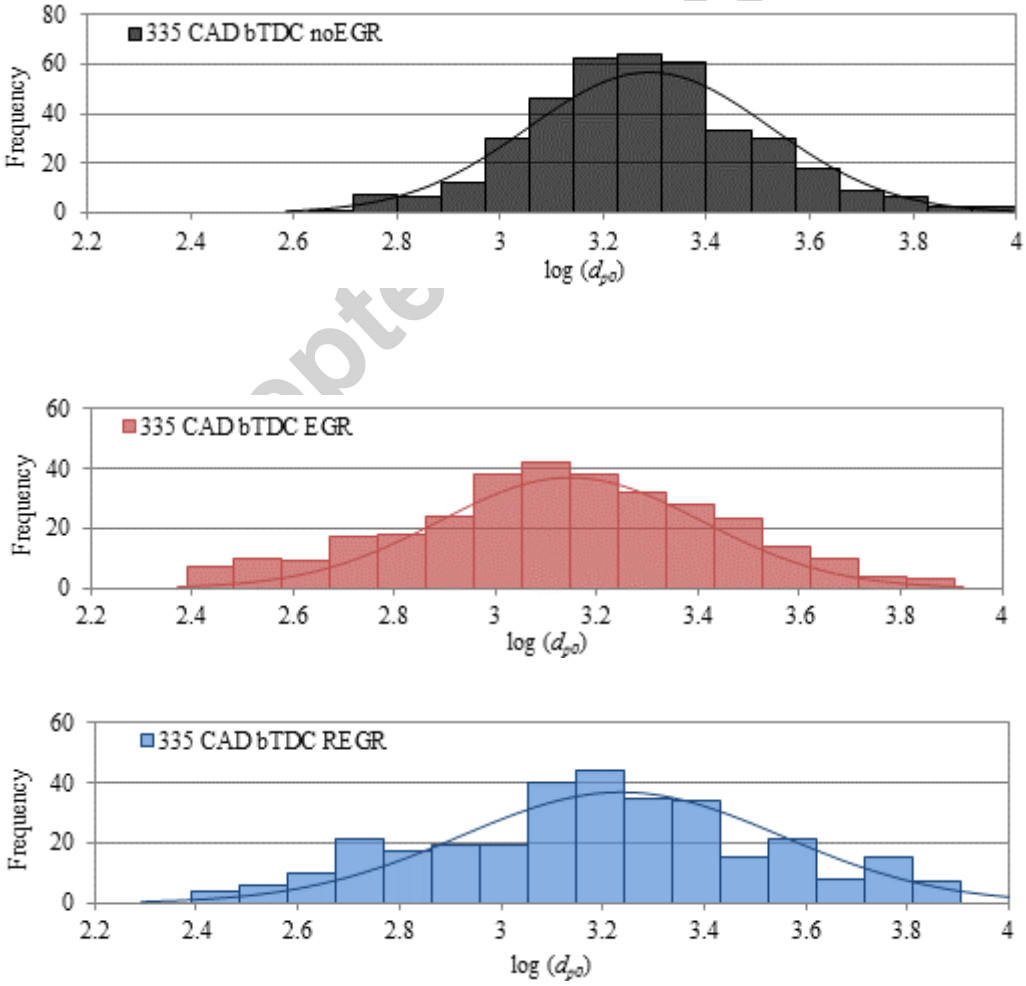

Figure 5. Primary particle size distribution for 335 CAD bTDC at noEGR, EGR and REGR.

EGR operation can lead to significant improvements in fuel economy and indicated efficiency (Fennell et al., 2014; Francqueville et al., 2014; Hedge et al., 2011). For REGR, this effect is even more pronounced (Fennell et al., 2014). The reduced quantity of liquid fuel in the combustion chamber and the reduction of the in-cylinder temperature as a result of the EGR addition with respect to the baseline operation (Fennell et al., 2014) could lead to lower rates of primary particle formation and growth, being responsible for the smaller sizes of primary particles. The engine operation with REGR slightly increases the diameter of the primary particle with respect to EGR despite the further reduction in quantity of the liquid fuel and the presence of hydrogen (Bogarra et al., 2016) in the combustion process that would have been expected to reduce the primary particle growth. Therefore, it is thought that the dominant effect responsible for the increase in the primary particle size with REGR with respect to EGR combustion is the hydrogen presence which could raise the local in-cylinder temperature increasing the rate of particle formation and counteracting the rest of the effects (i.e. chemical, thermal or dilution effects).

The effect of EGR on PM morphology has not been investigated in detail for GDI engines. However, for diesel, several studies have reported its influence on morphological characteristics. In (Lapuerta et al., 2007) no significant changes in d_{p0} were observed. The authors attributed this trend to a trade-off between the temperature levels and the lower oxygen concentration. Significant differences have been reported in soot microstructure from the EGR use when compared to baseline operation (Al-Qurashi et al., 2008). Soot produced under EGR showed higher reactivity (i.e. lower activation energy) and different oxidation patterns than the baseline soot. EGR soot oxidation presented a rapid internal burning which was not seen during the baseline soot oxidation. From the microstructure point of view, EGR increases the interlayer spacing in the soot and as a result increasing the likelihood of oxygen attack due to the less ordered structure. The disorder in the soot microstructure it is also attributed to a combination of thermal, chemical and dilution effects during the combustion process. Al-Qurashi et al. successfully separated the independent effects of CO_2 in EGR using a co-flow laminar flame burner fuelled with ethylene. The thermal effect was found to have the largest impact on soot reactivity. The higher heat capacity of CO_2 reduces the flame temperature. Furthermore, EGR modifies the graphite layer disposition favouring the oxygen attack and therefore, the increased presence of active sites (Al-Qurashi et al., 2011).

However, the authors did not find any impact of the soot's O/C ratio on its reactivity. Although, results and trends obtained for diesel engines can be extrapolated and adapted to modern gasoline engines, however the different mechanisms involved in soot formation with the use of EGR for both engines must be considered. While in diesel engines, EGR displaces part of the intake air, in gasoline, the air/fuel ratio is constant and therefore the mass of EGR is "added" to the mixture it is reducing the pumping losses, heat losses and the degree of dissociation in the burned gases (Ladommatos et al., 1998), also it is influencing the PM levels. However, in order to clarify the governing EGR mechanisms such as lower fuel presence in the combustion chamber, chemical, dilution or thermal effects, further analysis is needed.

The average diameter and standard deviation obtained from the primary PSD is represented in Figure 6. The 303 CAD bTDC fuel injection timing emits greater primary particles than the 335 CAD bTDC fuel injection timing as previously stated (Figure 4). Regarding the effect of EGR and REGR, the average diameters obtained were 27 nm, 23 nm and 25 nm at 335 CAD bTDC for noEGR, EGR and REGR, respectively. In in Figure 6, it can be seen that the standard deviation calculated from the primary particle sizes distribution overlaps. Therefore, to examine the significance of the EGR and REGR on the $d_{p0,}$ an independent sample T-test analysis has been performed. The significant level ($p<0.05$) indicated that the diameters are statistically different and therefore, particles emitted at noEGR are larger than those emitted under EGR and REGR operation.

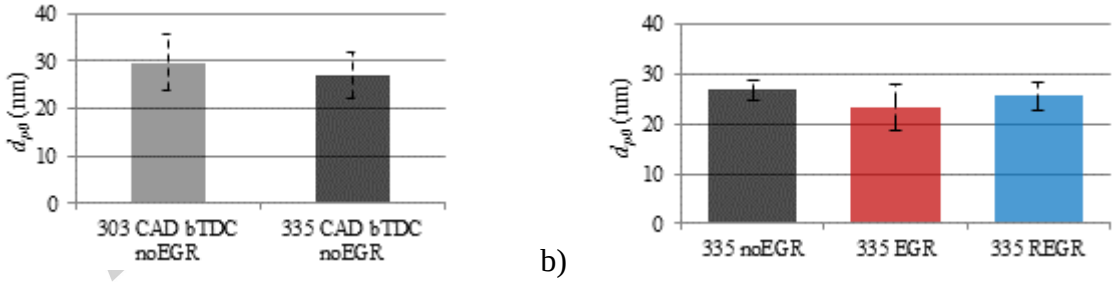

Figure 6. Average primary particle diameter: a) noEGR comparison at both injection timings (303 and 335 CAD bTDC) and b) noEGR, EGR and REGR at 335 CAD bTDC.

3.2.2. Number of primary particles and radius of gyration

To quantitatively understand the differences in PM morphology caused by the fuel injection timing, the number of primary particles n and the radius of gyration R_g are presented in Figure 7 for noEGR condition and in Figure 8 for EGR and REGR. At 303 CAD bTDC injection timing fewer number of agglomerates were found and this is in accordance with the

previously published scanning mobility particle sizer results (Bogarra et al., 2016). However, the presence of type b particles (Figure 1) increases the number of primary particles per agglomerate. Also, the variability (larger confidence intervals) at 303 CAD bTDC is higher than for 335 CAD bTDC.

The reason for these differences in PM morphology can be found in the diversity of the particle formation processes that are influenced by the fuel injection timings. In order to understand the mechanism governing PM formation and oxidation as well as the final exhaust-out emissions in GDI engines, optical techniques (Sementa et al., 2012; Stojkovic et al., 2005) and computational fluid dynamics (Bonatesta et al., 2014; Jiao et al., 2015; Köpple et al., 2015) have been used. It is agreed in the literature that the sources of PM formation are i) the presence of rich in fuel pockets during the combustion even in homogeneous mixtures ii) wall fuel-film formation due to fuel impingement and thus, pool fire and iii) carbonization of non-combusted fuel droplets (Bonatesta et al., 2014; Drake et al., 2003; Köpple et al., 2015; Song et al., 2015). The presence of pool fires is unavoidable in the wall-guided GDI engines (Song et al., 2015) and for gasoline engines the lack of oxygen can limit the oxidation of PM (Winklhofer et al., 2011). Furthermore, pool fires diffusive combustion begins late when the temperatures inside the chamber are low for soot oxidation (Stojkovic et al., 2005).

To understand soot formation mechanism in GDI engines, CFD analyses were carried out under advanced injection timings at different engine speeds (Bonatesta et al., 2014). It was shown that early injection produces fuel impingement and increases the concentration of fuel films in the piston crown, cylinder liner and cylinder head leading to pool fires and hence intense particle formation at the end of the combustion process. Delaying the injection timing to more homogeneous conditions (similar to 303 CAD bTDC in the present study) rich fuel vapour clouds in the combustion chamber free volume are reported to be the source of PM (Storch et al., 2015) and particularly the presence of rich fuel regions in the intake area (Song et al., 2015). Similar conclusions have been obtained in (Sementa et al., 2012) and (Jiao et al., 2015) for similar injection timings than the ones used in this work. The FSN was measured in a wide injection timing window, observing high smoke at advanced injection (>320 CAD bTDC) and reducing quickly after 305 CAD bTDC (Sementa et al., 2012). (Velji et al., 2010) found that for homogeneous mode, soot is formed in pool fires. In (Jiao et al., 2015) the fuel film mass and soot emissions are predicted using a multi-dimensional KIVA35V Release 2

code for CFD modelling. Although, heavy wetting of the piston head and liner was reported at advanced injection timings, there was no evidence of cylinder head wetting at retarded injection timing. In these rich in fuel regions, the temperature remained low hindering the oxidation of PM with OH radicals. Wall films produced under advanced injection timings remained liquid even during the late during the expansion stroke, a result that is opposite to the findings reported in (Stevens et al., 2001). In the latter investigation, no pool fires were observed for intake-strokes injection. However, different engine designs or injectors can lead to misleading comparisons (Drake et al., 2003). Also in (Drake et al., 2003) was discussed the link between fuel film thickness and smoke emissions. The authors claimed that a thin amount of wall film does not produce smoke as the fuel is evaporated before the pool fire formation or in the case that soot is formed, it will be oxidised. In stratified combustion, wetting of the spark plug is thought to be a considerable contributor to soot emissions (Hemdal et al., 2011). Similarly to the soot produced by early fuel injections, it is formed late in the combustion process where there are no OH radicals for soot oxidation. Recently, it has been investigated the most favourable conditions for soot formation in GDI engines (Hageman et al., 2015). The equivalence ratio threshold for soot formation in gasoline was found to lie between 1.3-1.4 and the temperature between 1400K-1700K. At early combustion stage, the temperature is higher than 2200K avoiding the formation of soot precursors. However, when the burned gases reach the piston or cylinder surfaces, the conditions are favourable for soot formation. The authors found a background level of PM is formed independently of the fuel used or the equivalence ratio despite homogenous condition and no wall-wetting conditions. The origin of this PM background is the lubricating oil and the engine wear.

According to the presented literature, at 335 CAD bTDC, a fuel film is formed in the piston crown, engine liner and even intake/exhaust valves due to the proximity of the piston to the TDC. The vaporization of the light components of the gasoline will leave the heavy fractions of the gasoline more prone to soot precursor formation in the expansion stroke (Drake et al., 2003; Jiao et al., 2015; Stevens et al., 2001) explaining the high concentration of soot at this early injection timing, 10 times higher (Bogarra et al., 2016). It is thought that at this injection timing, most of the agglomerates are formed in several regions late in the expansion stroke reducing the likelihood of collisions between the primary particles and agglomerates (less available time and larger volume when particles are formed) resulting in high density of agglomerates with lower number of primary particles than in 303 CAD bTDC injection

timing. On the other hand, at 303 CAD bTDC, although wall-wetting can still be produced, the mass of the fuel films will be lower and hence the particle matter formation. It is supposed that particles collected at 303 CAD bTDC injection timing could have been formed both near TDC (from rich pockets, references) and late in the expansion stroke (from wall wetting, references). Therefore, those particles were produced in small volumes of fuel rich regions and they had more available time for particle agglomeration. The increased number of primary particulates with larger diameters led to greater radius of gyration, however, the T-test results show that the difference in radius of gyration is not statistically significant. Thus, the calculation of D_f is needed to fully explain the trend.

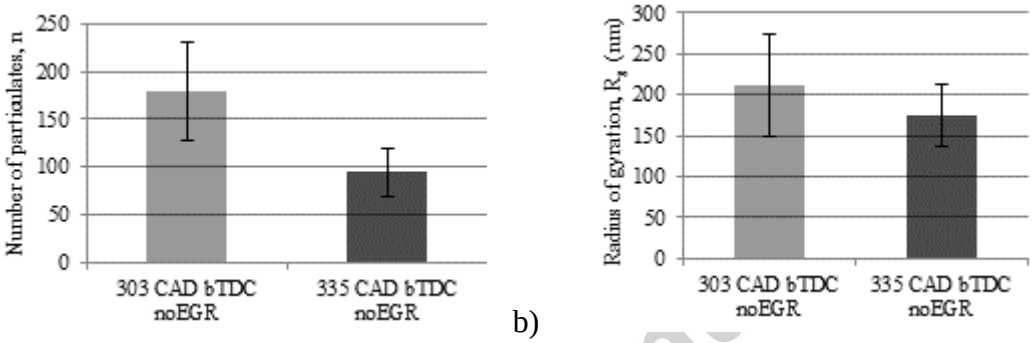

a) b)

Figure 7. Morphological parameters for the baselines: a) Number of particles per agglomerate and b) Radius of gyration (nm).

The effect of EGR and REGR on particle number was not found to be statistically significant, Figure 8. The confidence interval between the three conditions overlaps. Thus, the agglomerates are composed by a similar number of primary particles. However, the differences in primary particle size from baseline, EGR and REGR are reflected in the radius of gyration (Figure 8b). The noEGR condition presented the largest R_g while EGR and REGR showed similar values of R_g. These results are in agreement with the agglomerate mobility diameter findings reported elsewhere (Bogarra et al., 2016) meaning that EGR as well as REGR reduced PM formation and primary particles growth, but the agglomerates formed contain a similar number of primary particles. The reduction in particles size due to the hydrogen addition was also reported in (Choi et al., 2016) where an ethylene oppose jet counter diffusion flame configuration was used. They concluded that hydrogen addition led to i) the formation of fullerenic nanostructure (curved carbon lamella), ii) increased rate of acetylene (a well-known precursor) oxidation through OH oxidation which slow down benzene formation and therefore the development of large particles, iii) reduce soot surface growth through deactivation of soot surface site and iv) increase rate of 5-membered ring PAH which curves the fringes.

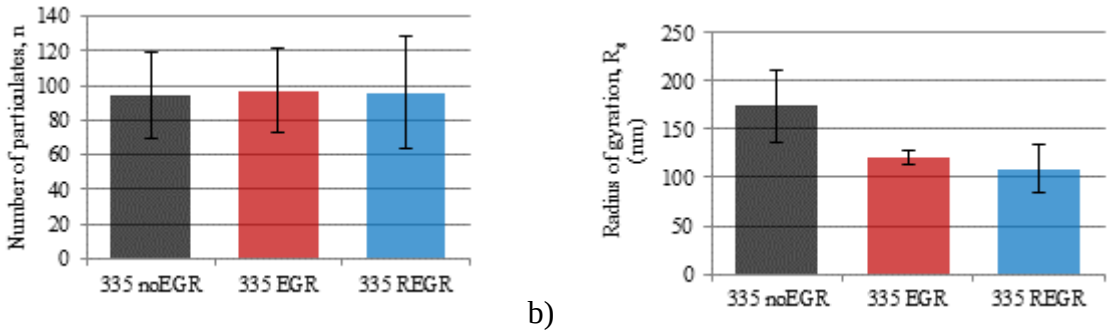

a) b)

Figure 8. Morphological parameters: a) Number of particles per agglomerate and b) Radius of gyration (nm).

3.2.3. Fractal dimension

The five different methods that are commonly used in the literature for the calculation of D_f are compared in this section and the results are presented in Figure 9. Even for diesel PM, there are not many papers that compared the values of D_f obtained from the different methods (Bushell et al., 2002). Calculating the fractal dimension with a logarithm method using the radius of gyration tends to underestimate its value, while using *LW* is being more accurate and sensitive to changes of engine operating condition. These methods provide an average value of D_f. per condition studied (noEGR, EGR and REGR) and therefore, a large number of micrographs have to be analysed in order to obtain accurate results. The rest of the three methods investigated here, provide a morphological value per agglomerate. The CBM showed little variation between samples while the iterative method and the RFF were the most susceptible to changes as it can be seen with the broader confidence level intervals.

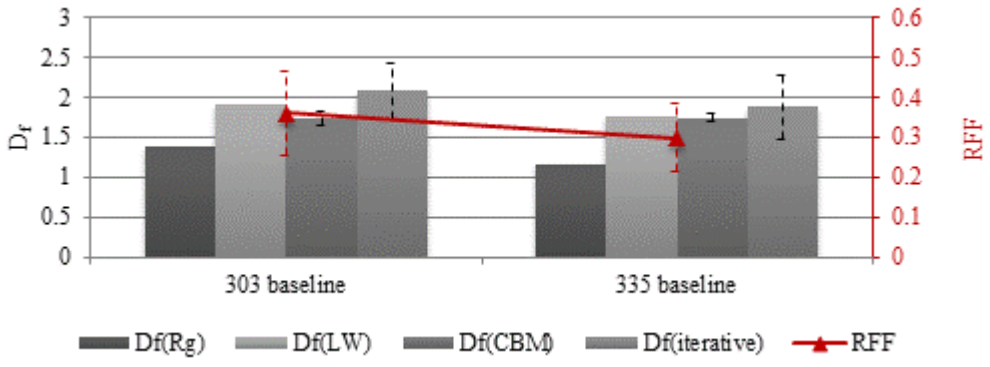

a)

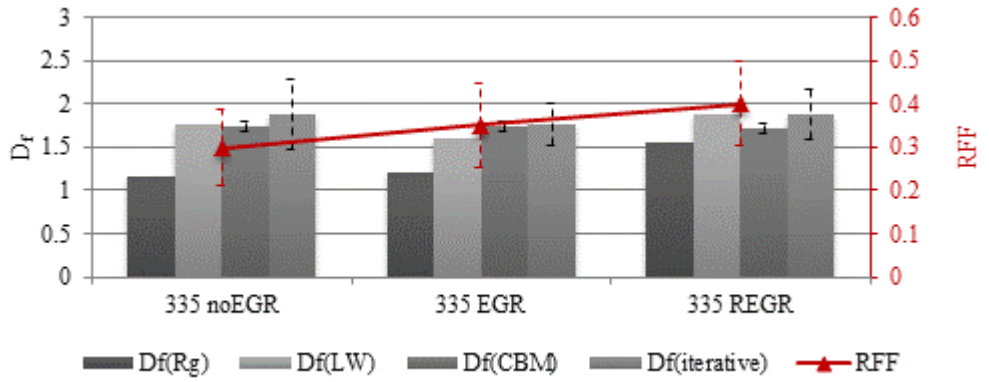

b)

Figure 9. Fractal dimension calculated using different methods: a) Baseline comparison and b) 335 CAD bTDC injection timing noEGR, EGR and REGR

With noEGR at 303 CAD bTDC fuel injection timing there are more compact agglomerates (i.e. higher D_f) than in the case of 335 CAD bTDC fuel injection timing, for all the methods compared in this investigation Figure 9a. The higher degree of compactness of the agglomerates emitted by 303 CAD bTDC explains the non-statistical differences in the R_g between the two injection timings, despite the larger number and size of primary particles hich form the agglomerates. Therefore, it can be concluded that the particles emitted at 303 CAD bTDC are composed of larger and higher number of primary particles than at 335 CAD bTDC, while those agglomerates are more compact.

The effect of EGR on the PM shape with respect to noEGR, Figure 9b, was within the confidence level intervals and no significant according to the T-test for the majority of the methods considered in this work. On the other hand, for all the methods except for the CBM, REGR tended to emit more compact/spherical particles (higher D_f and RFF) compared to the noEGR condition. Therefore REGR conditions emit agglomerates composed of a similar number of primary particles as the baseline condition, but the smaller primary particle size and more spherical shape resulted in smaller agglomerate average size. This higher fractal dimension increases the effective density and therefore the surface reactive area in contact with the lung fluid (Broday et al., 2011).

4. Conclusions

An analysis of PM morphology emitted by GDI engines has been carried out. Morphology parameters have been calculated for PM with different nature under noEGR, EGR and REGR conditions and statistical analyses have been performed to assure the significance of the results. Furthermore, different methodologies to calculate fractal dimension have been compared.

The outcomes show that at 303 CAD bTDC a variety of particle types are formed and higher variability in the results are obtained in contrast to 335 CAD, which produces particles similar to diesel ones. Additionally, the primary particle diameter and fractal dimension at 303 CAD bTDC are larger. Thus, under realistic GDI engine operation conditions, PM emitted has different characteristics than diesel, meaning that GPF design may differ from DPFs on account of the impact of morphological parameters in porosity and permeability. On the other hand, EGR reduced the average primary particle diameter and the radius of gyration maintaining the number of primary particles per agglomerate constant. The effect of REGR was similar, although the diameter was found to lie between noEGR and EGR conditions. Fractal dimension was not modified importantly under EGR conditions. In the case of EGR, depending on the method, different trends can be obtained and the difference was not found statistically significant. However, REGR increased the fractal dimension value when compared to no EGR conditions. Although at REGR fewer particles are produced, the smaller diameter and larger fractal dimension can reduce the filtration efficiency and increase the hazardous impact for human health. Therefore, the aftertreatment systems will need to be improved.

These findings can aid in the optimization of engine parameters which can modify the morphology parameters for the effective design of aftertreatment systems, reducing the number and the aggressiveness of the regeneration processes and decreasing the deposition rate in human body. In order to completely understand the soot interactions in the aftertreatment devices and their impact in human health, the soot reactivity must be analysed. Thus, further research of the microstructure, intimately linked with the soot oxidation process together with the already presented morphology studied is needed.

ACKNOWLEDGMENTS

The authors would like to thank EPSRC (Grant Number: 1377213) and Johnson Matthey for funding the project and providing a scholarship to Maria Bogarra. Innovate UK (Technology Strategy Board) is acknowledged for supporting this work with the project "CO_2 Reduction through Emissions Optimisation" (CREO: ref. 400176/149) in collaboration with Ford Motor Company, Jaguar Land Rover and Cambustion. The Advantage West Midlands and the European Regional Development Fund as part of the Science City Research Alliance Energy Efficiency Project are also acknowledged for supporting the research work. Mrs Theresa Morris is also thanked for her kind support in obtaining the TEM micrographs.

References

Akif Ceviz, M., Sen, A. K., Küleri, A. K., & Volkan Öner, İ. (2012). Engine performance, exhaust emissions, and cyclic variations in a lean-burn SI engine fueled by gasoline–hydrogen blends. *Applied Thermal Engineering, 36*, 314-324. doi: 10.1016/j.applthermaleng.2011.10.039

Al-Qurashi, K., & Boehman, A. L. (2008). Impact of exhaust gas recirculation (EGR) on the oxidative reactivity of diesel engine soot. *Combustion and Flame, 155*(4), 675-695. doi: 10.1016/j.combustflame.2008.06.002

Al-Qurashi, K., Lueking, A. D., & Boehman, A. L. (2011). The deconvolution of the thermal, dilution, and chemical effects of exhaust gas recirculation (EGR) on the reactivity of engine and flame soot. *Combustion and Flame, 158*(9), 1696-1704. doi: 10.1016/j.combustflame.2011.02.006

Alger, T., & Mangold, B. (2009). Dedicated EGR: A New Concept in High Efficiency Engines. *SAE Int. J. Engines, 2009-01-0694, 2*(1).

Badshah, H., & Khalek, I. (2015). Solid Particle Emissions from Vehicle Exhaust during Engine Start-Up. *SAE Int. J. Engines, 8*(4), 1492-1502. doi: 10.4271/2015-01-1077

Barone, T. L., Storey, J. M. E., Youngquist, A. D., & Szybist, J. P. (2012). An analysis of direct-injection spark-ignition (DISI) soot morphology. *Atmospheric Environment, 49*, 268-274. doi: 10.1016/j.atmosenv.2011.11.047

Bogarra, M., Herreros, J. M., Tsolakis, A., York, A., & Millington, P. (2016). Characterization of particulate matter sampling system and emissions from a gasoline direct injection (GDI) engine with fuel reforming. . *SAE Int. J. Engines, 9*(1). doi: 10.4271/2015-01-2019

Bonatesta, F., La Rocca, S., Hopkins, E., & Bell, D. (2014). Application of Computational Fluid Dynamics to Explore the Sources of Soot Formation in a Gasoline Direct Injection Engine. *1*. doi: 10.4271/2014-01-2569

Broday, D. M., & Rosenzweig, R. (2011). Deposition of fractal-like soot aggregates in the human respiratory tract. *Journal of Aerosol Science, 42*(6), 372-386. doi: 10.1016/j.jaerosci.2011.03.001

Bushell, G. C., Yan, Y. D., Woodfields, D., Raper, J., & Amal, R. (2002). On techniques for the measurement of the mass fractal dimension of aggregates. *Advances in Colloid and Interface Science, 95*(1), 1-50. doi: 10.1016/S0001-8686(00)00078-6

Chadwell, C., Alger, T., Zuehl, J., & Gukelberger, R. (2014). A Demonstration of Dedicated EGR on a 2.0 L GDI Engine. *SAE International Journal of Engines, 7*(1), 434-447. doi: 10.4271/2014-01-1190

Choi, J.-H., Hwang, C.-H., Choi, S. K., Lee, S. M., Lee, W. J., Jang, S. H., & Park, S.-H. (2016). Impacts of hydrogen addition on micro and nanostructure of soot particles formed in C2H4/air counter diffusion flames. *International Journal of Hydrogen Energy*. doi: 10.1016/j.ijhydene.2016.04.158

Drake, M., Fansler, T., Solomon, A., & Szekely, G. (2003). Piston Fuel Films as a Source of Smoke and Hydrocarbon Emissions from a Wall-Controlled Spark-Ignited Direct-Injection Engine,. *SAE Technical Paper 2003-01-0547*. doi: 10.4271/2003-01-0547

Farron, C., Matthias, N., Foster, D., Andrie, M., R., K., & Najt, P. (2011). Particulate Characteristics for Varying Engine Operation in a Gasoline Spark Ignited, Direct Injection Engine. *SAE Technical Paper, 2011-01-1220*. doi: 10.4271/2011-01-1220.

Fennell, D., Herreros, J., & Tsolakis, A. (2014). Improving gasoline direct injection (GDI) engine efficiency and emissions with hydrogen from exhaust gas fuel reforming. *International Journal of Hydrogen Energy, 39*(10), 5153-5162. doi: 10.1016/j.ijhydene.2014.01.065

Fennell, D., Herreros, J., Tsolakis, A., Cockle, K., Pignon, J., & Millington, P. (2015). Thermochemical recovery technology for improved modern engine fuel economy – part 1: analysis of a prototype exhaust gas fuel reformer. *RSC Adv., 5*(44), 35252-35261. doi: 10.1039/c5ra03111g

Fennell, D., Herreros, J., Tsolakis, A., & Xu, H. (2013). GDI Engine Performance and Emissions with Reformed Exhaust Gas Recirculation (REGR). *SAE Technical Paper, 2013-01-0537*. doi: 10.4271/2013-01-0537.

Filippov, A. V., Zurita, M., & Rosner, D. E. (2000). Fractal-like Aggregates: Relation between Morphology and Physical Properties. *J Colloid Interface Sci, 229*(1), 261-273. doi: 10.1006/jcis.2000.7027

Fiorito, S., Mastrofracesco, A., Cardinali, G., Rosato, E., Salsano, F., Su, D. S., . . . Picardo, M. (2011). Effects of carbonaceous nanoparticles from low-emission and older diesel engines on human skin cells. *Carbon, 49*(15), 5038-5048. doi: 10.1016/j.carbon.2011.07.022

Francqueville, L., & Michel, J.-B. (2014). On the Effects of EGR on Spark-Ignited Gasoline Combustion at High Load. *SAE International Journal of Engines, 7*(4), 1808-1823. doi: 10.4271/2014-01-2628

Gaddam, C. K., & Vander Wal, R. L. (2013). Physical and chemical characterization of SIDI engine particulates. *Combustion and Flame, 160*(11), 2517-2528. doi: 10.1016/j.combustflame.2013.05.025

Giechaskiel, B., Alföldy, B., & Drossinos, Y. (2009). A metric for health effects studies of diesel exhaust particles. *Journal of Aerosol Science, 40*(8), 639-651. doi: 10.1016/j.jaerosci.2009.04.008

Hageman, M. D., Sakai, S. S., & Rothamer, D. A. (2015). Determination of soot onset and background particulate levels in a spark-ignition engine. *Proceedings of the Combustion Institute, 35*(3), 2949-2956. doi: 10.1016/j.proci.2014.06.105

Hedge, M., Weber, P., Gingrich, J., Alger, T., & Khalek, I. A. (2011). Effect of EGR on Particle Emissions from a GDI Engine. *SAE Int. J. Engines, 4*(1), 650-666. doi: 10.4271/2011-01-0636

Hemdal, S., Andersson, M., Dahlander, P., Ochoterena, R., & Denbratt, I. (2011). In-cylinder soot imaging and emissions of stratified combustion in a spark-ignited spray-guided direct-injection gasoline engine. *International Journal of Engine Research, 12*(6), 549-563. doi: 10.1177/1468087411418167

Henry, C., Kroll, S., Premnath, V., Smith, I., Morgan, P., & Khalek, I. (2016). Detailed Characterization of Criteria Pollutant Emissions from D-EGR®Light Duty Vehicle. *1*. doi: 10.4271/2016-01-1006

Jiao, Q., & Reitz, R. D. (2015). The Effect of Operating Parameters on Soot Emissions in GDI Engines. *SAE International Journal of Engines, 2015-01-1071*. doi: 10.4271/2015-01-1071

Karjalainen, P., Pirjola, L., Heikkilä, J., Lähde, T., Tzamkiozis, T., Ntziachristos, L., . . . Rönkkö, T. (2014). Exhaust particles of modern gasoline vehicles: A laboratory and an on-road study. *Atmospheric Environment, 97*, 262-270. doi: 10.1016/j.atmosenv.2014.08.025

Kondo, K., Aizawa, T., Kook, S., & Pickett, L. (2013). Uncertainty in Sampling and TEM Analysis of Soot Particles in Diesel Spray Flame. *SAE Technical Paper, 2013-01-0908*. doi: 10.4271/2013-01-090

Köpple, F., Jochmann, P., Hettinger, A., Kufferath, A., & Bargende, M. (2015). A Novel CFD Approach for an Improved Prediction of Particulate Emissions in GDI Engines by Considering the Spray-Cooling on the Piston. *1*. doi: 10.4271/2015-01-0385

La Rocca, A., Bonatesta, F., Fay, M. W., & Campanella, F. (2015). Characterisation of soot in oil from a gasoline direct injection engine using Transmission Electron Microscopy. *Tribology International, 86*, 77-84. doi: 10.1016/j.triboint.2015.01.025

Ladommatos, N., Abdelhalim, S., Zhao, H., & Hu, Z. (1998). The effects of carbon dioxide in exhaust gas recirculation on diesel engine emissions. . *P I MECH ENG D-J AUT 212*, 25 - 42.

Lapuerta, M., Ballesteros, R., & Martos, F. J. (2006). A method to determine the fractal dimension of diesel soot agglomerates. *J Colloid Interface Sci, 303*(1), 149-158. doi: 10.1016/j.jcis.2006.07.066

Lapuerta, M., Martos, F. J., & Herreros, J. M. (2007). Effect of engine operating conditions on the size of primary particles composing diesel soot agglomerates. *Journal of Aerosol Science, 38*(4), 455-466. doi: 10.1016/j.jaerosci.2007.02.001

Lapuerta, M., Oliva, F., & Martínez-Martínez, S. (2010). Modeling of the Soot Accumulation in DPF Under Typical Vehicle Operating Conditions *SAE Int. J. Fuels Lubr. , 3*(2), 532-542. doi: 10.4271/2010-01-2097

Lee, K., Seong, H., Sakai, S., Hageman, M., & Rothamer, D. (2013). Detailed Morphological Properties of Nanoparticles from Gasoline Direct Injection Engine Combustion of Ethanol Blends. *SAE Technical Paper, 2013-24-0185*. doi: 10.4271/2013-24-0185.

Löndahl, J., Massling, A., Swietlicki, E., Bräuner, E. V., Ketzel, M., Pagels, J., & Loft, S. (2009). Experimentally Determined Human Respiratory Tract Deposition of Airborne Particles at a Busy Street. *Environ. Sci. Technol., 43*(13), 4659–4664. doi: 10.1021/es803029b

Lottin, D., Ferry, D., Gay, J. M., Delhaye, D., & Ouf, F. X. (2013). On methods determining the fractal dimension of combustion aerosols and particleclusters. *Journal of Aerosol Science, 58*, 41-49. doi: 10.1016/j.jaerosci.2012.12.009

Maricq, M. M. (2007). Coagulation dynamics of fractal-like soot aggregates. *Journal of Aerosol Science, 38*(2), 141-156. doi: 10.1016/j.jaerosci.2006.11.004

Miyashita, K., Fukuda, Y., Shiozaki, Y., & Kondo, K. (2015). TEM Analysis of Soot Particles Sampled from Gasoline Direction Injection Engine Exhaust at Different Fuel Injection Timings. *SAE Technical Paper 2015-01-1872*. doi: 10.4271/2015-01-1872.

Ruiz, F. A., Lopez, A. F., & Agudelo, J. R. (2015). Morphological characteristics and fractal analysis of diesel particulate matter from TEM images produced by dual-fuel n-butanol injection.

Proceedings of the ASME 2015 International Mechanical Engineering Congress and Exposition

Schaefer, D. W. (1988). Fractal Models and the Structure of Materials. *MRS Bulletin, 13*, pp 22-27. doi: doi:10.1557/S088376940006632X

Sementa, P., Maria Vaglieco, B., & Catapano, F. (2012). Thermodynamic and optical characterizations of a high performance GDI engine operating in homogeneous and stratified charge mixture conditions fueled with gasoline and bio-ethanol. *Fuel, 96*, 204-219. doi: 10.1016/j.fuel.2011.12.068

Seong, H., Lee, K., & Choi, S. (2013). Effects of Engine Operating Parameters on Morphology of Particulates from a Gasoline Direct Injection (GDI) Engine. *SAE Technical Paper, 2013-01-2574*. doi: 10.4271/2013-01-2574.

Song, J., Kim, T., Jang, J., & Park, S. (2015). Effects of the injection strategy on the mixture formation and combustion characteristics in a DISI (direct injection spark ignition) optical engine. *Energy, 93*, 1758-1768. doi: 10.1016/j.energy.2015.10.058

Stevens, E., & Steeper, R. (2001). Piston Wetting in an Optical DISI Engine: Fuel Films, Pool Fires, and Soot Generation,. *SAE Technical Paper 2001-01-1203*. doi: 10.4271/2001-01-1203

Stojkovic, B. D., Fansler, T. D., Drake, M. C., & Sick, V. (2005). High-speed imaging of OH* and soot temperature and concentration in a stratified-charge direct-injection gasoline engine. *Proceedings of the Combustion Institute, 30*(2), 2657-2665. doi: 10.1016/j.proci.2004.08.021

Stone, R., Zhao, H., & Zhou, L. (2010). Analysis of Combustion and Particulate Emissions when Hydrogen is Aspirated into a Gasoline Direct Injection Engine. *SAE Technical Paper, 2010-01-0580*. doi: 10.4271/2010-01-0580

Storch, M., Hinrichsen, F., Wensing, M., Will, S., & Zigan, L. (2015). The effect of ethanol blending on mixture formation, combustion and soot emission studied in an optical DISI engine. *Applied Energy, 156*, 783-792. doi: 10.1016/j.apenergy.2015.06.030

Theiler, J. (1990). Estimating Fractal Dimenstion. *Journal of the Optical Society of America A, 7*(6), 1055-1073. doi: 10.1364/JOSAA.7.001055

Uy, D., Ford, M. A., Jayne, D. T., O'Neill, A. E., Haack, L. P., Hangas, J., . . . Gangopadhyay, A. K. (2014). Characterization of gasoline soot and comparison to diesel soot: Morphology, chemistry, and wear. *Tribology International, 80*, 198-209. doi: 10.1016/j.triboint.2014.06.009

Van Gulijk, C., Marijnissen, J. C. M., Makkee, M., Moulijn, J. A., & Schmidt-Ott, A. (2004). Measuring diesel soot with a scanning mobility particle sizer and an electrical low-pressure impactor: performance assessment with a model for fractal-like agglomerates. *Journal of Aerosol Science, 35*(5), 633-655. doi: 10.1016/j.jaerosci.2003.11.004

Vander Wal, R. L., Yezerets, A., Currier, N. W., Kim, D. H., & Wang, C. M. (2007). HRTEM Study of diesel soot collected from diesel particulate filters. *Carbon, 45*(1), 70-77. doi: 10.1016/j.carbon.2006.08.005

Velji, A., Yeom, K., Wagner, U., & Spicher, U. (2010). Investigations of the Formation and Oxidation of Soot Inside a Direct Injection Spark Ignition Engine Using Advanced Laser-Techniques. *SAE Technical Paper, 2010-01-0352*. doi: 10.4271/2010-01-0352

Verhelst, S., & Wallner, T. (2009). Hydrogen-fueled internal combustion engines. *Progress in Energy and Combustion Science, 35*(6), 490-527. doi: 10.1016/j.pecs.2009.08.001

Wang-Hansen, C., Ericsson, P., Lundberg, B., Skoglundh, M., Carlsson, P.-A., & Andersson, B. (2013). Characterization of Particulate Matter from Direct Injected Gasoline Engines. *Topics in Catalysis, 56*(1-8), 446-451. doi: 10.1007/s11244-013-9994-4

Wentzel, M., Gorzawski, H., Naumann, K. H., Saathoff, H., & Weinbruch, S. (2003). Transmission electron microscopical and aerosol dynamical characterization of soot aerosols. *Journal of Aerosol Science, 34*(10), 1347-1370. doi: 10.1016/s0021-8502(03)00360-4

Winklhofer, E., Neubauer, M., Hirsch, A., & Philipp, H. (2011). Cylinder- and Cycle Resolved Particle Formation Evaluation to Support GDI Engine Development for Euro 6 Targets. *1*. doi: 10.4271/2011-24-0206

Wozniak, M., Onofri, F. R. A., Barbosa, S., Yon, J., & Mroczka, J. (2012). Comparison of methods to derive morphological parameters of multi-fractal samples of particle aggregates from TEM images. *Journal of Aerosol Science, 47*, 12-26. doi: 10.1016/j.jaerosci.2011.12.008

Zhang, S., & McMahon, W. (2012). Particulate Emissions for LEV II Light-Duty Gasoline Direct Injection Vehicles. *SAE International Journal of Fuels and Lubricants, 5*(2), 637-646. doi: 10.4271/2012-01-0442

Zhu, J., Lee, K., Yozgatligil, A., & Choi, M. Y. (2005). Effects of engine operating conditions on morphology, microstructure, and fractal geometry of light-duty diesel engine particulates. *Proceedings of the Combustion Institute, 30*(2), 2781-2789. doi: 10.1016/j.proci.2004.08.232

Highlights

- The morphology of different types of particulates emitted by a modern GDI has been characterised.
- The influence of reformate combustion on particulate matter (PM) morphology has been studied.
- Relevant methods to analyse the shape of the particulates (i.e. fractal dimension) have been assessed.